Original Research

T_2 Relaxometry of Normal Pediatric Brain Development

Ilana R. Leppert, MEng,[1]* C. Robert Almli, PhD,[2] Robert C. McKinstry, MD, PhD,[3] Robert V. Mulkern, PhD,[4] Carlo Pierpaoli, MD, PhD,[5] Michael J. Rivkin, MD,[6] G. Bruce Pike, PhD,[1] and the Brain Development Cooperative Group

Purpose: To establish normal age-related changes in the magnetic resonance (MR) T_2 relaxation time constants of brain using data collected as part of the National Institutes of Health (NIH) MRI Study of Normal Brain Development.

Materials and Methods: This multicenter study of normal brain and behavior development provides both longitudinal and cross-sectional data, and has enabled us to investigate T_2 evolution in several brain regions in healthy children within the age range of birth through 4 years 5 months. Due to the multicenter nature of the study and the extended period of data collection, periodically scanned inanimate and human phantoms were used to assess intra- and intersite variability.

Results: The main finding of this work, based on over 340 scans, is the identification and parameterization of the monoexponential evolution of T_2 from birth through 4 years 5 months of age in various brain structures.

Conclusion: The exponentially decaying T_2 behavior is believed to reflect the rapid changes in water content as well as myelination during brain development. The data will become publicly available as part of a normative pediatric MRI and clinical/behavioral database, thereby providing a basis for comparison in studies assessing normal brain development, and studies of deviations due to various neurological, neuropsychiatric, and developmental disorders.

Key Words: T_2 relaxometry; pediatric; brain development; myelination; multicenter
J. Magn. Reson. Imaging 2009;29:258–267.

QUANTITATIVE MRI ACQUISITION and analysis techniques allow investigations beyond the conventional qualitative interpretation employed in routine clinical practice. Such approaches are aimed at quantifying specific tissue characteristics, providing reproducible indices mirroring the underlying biological system. Relaxometry, for instance, combines acquisition and analysis techniques to generate MR relaxation time constants that directly reflect the local environment of protons. In particular, given its sensitivity to alterations in tissue microstructure, T_2 relaxation provides a quantitative monitoring tool in both health and disease conditions.

Previous studies examined brain development by assessing gray matter (GM) and white matter (WM) contrast variations observed in early childhood (1–4). These qualitative contrast assessments examined conventional T_1-weighted (T_1W) and T_2-weighted (T_2W) images, were often acquired in the context of clinical examinations, and retained only those subjects who were deemed to have no neurological pathology (1). Some of these studies presented more quantitative GM/WM contrast ratios that clearly captured the well-known qualitative contrast change associated with the stages of myelination (2,4).

The finding that GM and WM contrast in infancy is reversed compared to that of adults is striking. This reversed contrast is observed during the first 4–6 months postnatal, and the change to the adult pattern occurs at around the age of 9–12 months (5). The actual timing of the contrast reversal is dependent on the field

[1]Montreal Neurological Institute, McGill University, Montreal, Quebec, Canada.
[2]Developmental Neuropsychobiology Laboratory, Departments of Neurology, Psychology, Programs in Neuroscience, Occupational Therapy, Washington University, School of Medicine, St. Louis, Missouri, USA.
[3]Mallinckrodt Institute of Radiology and St. Louis Children's Hospital, Washington University Medical Center, St. Louis, Missouri, USA.
[4]Department of Radiology, Children's Hospital, Harvard Medical School, Boston, Massachusetts, USA.
[5]National Institute of Child Health and Human Development, National Institutes of Health, Bethesda, Maryland, USA.
[6]Departments of Neurology, Psychiatry and Radiology, Children's Hospital, Harvard Medical School, Boston, Massachusetts, USA.
Contract grant sponsor: National Institute of Child Health and Human Development; Contract grant number: N01-HD02-3343; Contract grant sponsor: National Institute of Mental Health; Contract grant number: N01-MH9-0002; Contract grant sponsor: National Institute of Neurological Disorders and Stroke; Contract grant numbers: N01-NS-9-2314, N01-NS-9-2315, N01-NS-9-2316, N01-NS-9-2317, N01-NS-9-2319, N01-NS-9-2320; Contract grant sponsor: National Institute on Drug Abuse; Contract grant sponsor: NIH Neuroscience Blueprint.
*Address reprint requests to: I.R.L., Montreal Neurological Institute, 3801 University St., WB325, Montreal, Quebec, Canada, H3A 2B4. E-mail: ilana@bic.mni.mcgill.ca
Received October 3, 2007; Accepted October 7, 2008.
DOI 10.1002/jmri.21646
Published online in Wiley InterScience (www.interscience.wiley.com).

strength, the imaging sequence, and the brain region studied (3). These qualitative contrast changes stem from the governing relaxation parameters, T_1 and T_2, as well as from the proton density (PD), which all reflect microstructural changes associated with maturation of the underlying tissue. Ideally, a quantitative relaxometry approach to assessing maturation would avoid imaging-sequence dependence and permit the detection of changes earlier and more consistently than qualitative methods (6).

A consistent observation throughout quantitative relaxometry studies is prolonged relaxation times in neonates, followed by a steep decline in both T_1 and T_2 values, especially during the first year of life. Subsequently, a slower decrease extends into the third year, at which age the relaxation parameters approach adult values (5–9). Because the rate of T_2 shortening is much faster than that observed for T_1, it is assumed that T_2 is more sensitive to tissue changes and is therefore often preferred as an index of early brain development (10).

In many previous studies, cohorts originated from clinical investigations, and data collection was limited to infants who showed no apparent MR abnormalities. Thus, the study subjects were not necessarily samples of a strictly normal, healthy population. Recognizing this need for data encompassing populations of normal, healthy young children, the National Institutes of Health (NIH) sponsored a multicenter study entitled the MRI Study of Normal Brain Development (also known as the NIH Pediatric MRI Data Repository, when referring to the database) (11), for which recruitment is demographically diverse and representative of the U.S. population in terms of gender, race and ethnicity, and family income. This NIH study consisted of examining approximately 500 children over a seven-year period, with two distinct objectives, partitioned by age groups: 4.5–18 years (Objective 1), and birth to 4 years 5 months (Objective 2).

The data acquisition included several domains, each aimed at monitoring different aspects of development, such as gross morphological changes via anatomical MRI, biochemical characteristics using MR spectroscopy, tissue microstructure through diffusion tensor imaging, and relaxometry (Objective 2 only), as well as behavioral and cognitive development with the aid of a large battery of age-appropriate neurological and neuropsychological tests. The ultimate goal of this project is to provide a publicly available normative pediatric MRI brain and behavioral database that can subsequently be used in studies assessing normal brain development and brain deviations associated with neurological, neuropsychiatric, and developmental disorders (11). The objectives of the present work were to estimate T_2 values in several brain regions in 344 brain scans of a representative group of healthy children aged birth through 4 years 5 months of age, and to subsequently model the evolution of the T_2 relaxation time constant with age.

MATERIALS AND METHODS

Subject Cohort

As part of the Objective 2 age range (birth through 4 years 5 months) of the NIH pediatric study, 114 normal, healthy children were recruited, across 11 age cohorts as described by Almli et al (12). These cohorts are characterized by predetermined ages at which the children began the study, providing a cross-sectional component of the study, while the longitudinal component was achieved with at least two additional visits, i.e., a minimum of three scanning sessions for each child (excluding subject attrition). In addition, the demographically balanced sampling plan was governed by three other factors, namely gender (approximately the same number of males and females), family income, and race/ethnicity based on data from the U.S. Census Bureau (13). For each of these subjects, MRI, neurological, and behavioral data were collected as described in detail elsewhere (11).

Table 1
Age and Gender Distribution of Subject Scans at Each Data Collection Site

Age range (months)	S1 (male/female)	S2 (male/female)	Total (male/female)
0	13 (6/7)	10 (2/8)	23 (8/15)
3	7 (4/3)	22 (13/9)	29 (17/12)
6	16 (10/6)	25 (10/15)	41 (20/21)
9	15 (7/8)	24 (11/13)	39 (18/21)
12	9 (5/4)	25 (12/13)	34 (17/17)
15	7 (6/1)	25 (11/14)	32 (17/15)
18	8 (5/3)	32 (16/16)	40 (21/19)
24	5 (4/1)	22 (14/8)	27 (18/9)
30	4 (2/2)	27 (17/10)	31 (19/12)
36	4 (1/3)	21 (10/11)	25 (11/14)
48	3 (1/2)	20 (11/9)	23 (12/11)
Total	91 (51/40)	253 (127/126)	344 (178/166)

S1 = site 1, S2 = site 2.

Table 1 summarizes the MRI T_2 relaxometry data collected for each of the two participating sites: site 1 (S1) and site 2 (S2). A total of 114 subjects (total [male/female]; S1: 45 27/18; S2: 69 40/29) and 344 scans were completed. A shorter interval sampling plan was chosen for the younger subjects (238 brains scans between the age of 0 and 18 months [i.e., 3-month interscan intervals]) vs. older subjects (106 scans between 18 months to 53 months [i.e., 6-month or 12-month interscan intervals]) in order to capture the rapid developmental changes expected during early infancy (14).

Relaxometry Protocols and T_2 Estimation

With the goal of estimating the T_2 relaxation time, two dual-contrast turbo spin-echo (TSE) acquisitions were carried out on 1.5 Tesla systems (GE Signa at S1 and Siemens Sonata at S2). The acquisition time of each set of dual-contrast images was about 3–5 minutes with a $1 \times 1 \times 3$ mm resolution, using the following timing parameters (TR/TE1/TE2; TR/TE3/TE4) and fields of view (FOVs): [GE: 3500/14/112 msec; 3500/83/165 msec, FOV: 256×256 mm] [Siemens: 3500/13/121 msec; 3500/83/165 msec, FOV: 256×256 mm]. The second dual-contrast acquisition, with longer TE values, provides stronger T_2-weighting and increased sensitivity to the longer relaxation times expected in young infants. The T_2 estimates generated from two to four effective echo times (TEs) in standard TSE sequences,

utilizing two-dimensional Fourier transform (2D-FT) multislice techniques with slice-selective 90° and 180° pulses, suffer from systematic errors due to the introduction of signal from stimulated echoes and other echo pathways. More accurate T_2 measurements can be sought using more rigorous pulse sequence strategies, as discussed by Poon and Henkelman (15). Such strategies have been employed in other studies, in single slice mode and with much longer scan times, to assess multiexponential T_2 signal decay curves that may reflect, for example, short T_2 components from myelin-associated water as well as longer T_2 components from other intra- and extracellular water compartments (16). The long scan times and limited volume coverage associated with such truly accurate T_2 characterizations preclude, in our view, their incorporation into this study of unsedated children under 5 years of age. Furthermore, the T_2 values we report are sensitive to age-related changes in tissue water content and distribution, and are actually more relevant than "true" T_2 values when considering and/or predicting brain tissue contrast observed clinically when using the most widely adopted T_2W imaging technique in the world.

Through the NIH pediatric study protocol, all children were scanned during natural sleep (i.e., without sedation) using anatomical T_1W and PD/T_2W scans followed by T_1 relaxometry acquisitions, then either diffusion tensor imaging or MR spectroscopy, and finally the additional T_2 relaxometry scans, for a total scan time of less than one hour. The neuroanatomical scans (T_1W and PD/T_2W) are the highest priority and a scanning session is only deemed successful if these acquisitions are completed (11). It is also evident from this prioritized list of acquisitions that the second set of T_2W images was acquired toward the end of the protocol, increasing the likelihood that the subject would be unable to complete the entire data collection. T_2 maps were calculated using either two or four TEs, via the following linearized equation:

$$S_i = S_0 e^{-TE/T_2} \Rightarrow \ln(S_i) = \ln(S_0) - \frac{TE_i}{T_2}, \qquad [1]$$

where S_0 is the equilibrium signal and S_i is the signal at the i^{th} TE (TE_i). The linear regressions were carried out using MATLAB (The Mathworks, Inc., Natick, MA, USA).

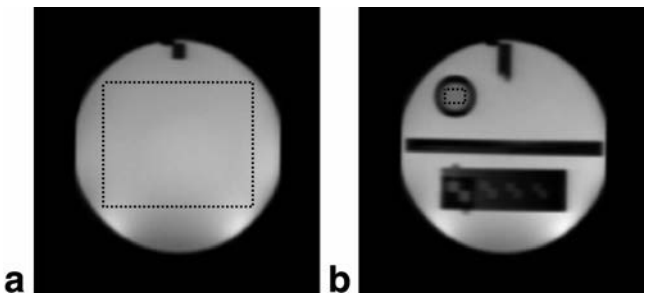

Figure 1. ROI selection for the ACR phantom, indicated by dotted lines. **a:** (ROI 1) Main compartment: 10 mmol NiCl, 75 mmol NaCl, $T_2 \sim 125$ msec. **b:** (ROI 2) Contrast vial: 20 mmol NiCl, 15 mmol NaCl, $T_2 \sim 70$ msec.

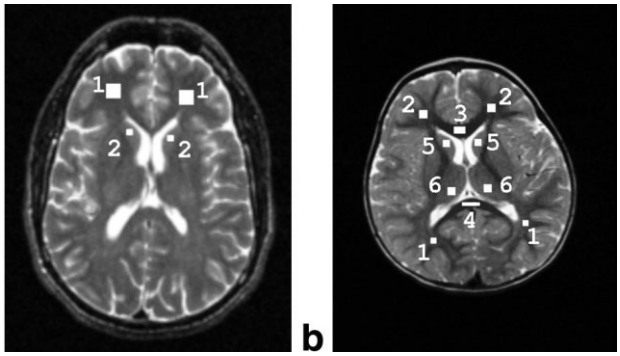

Figure 2. ROI selection for (**a**) living phantom: 1) ROI 1: frontal WM; $T_2 \sim 80$–90 msec, 2) ROI 2: head of caudate nucleus; $T_2 \sim$ 90–100 msec; and (**b**) subjects (shown here on a T_2W image of a 52-month-old subject) in WM: 1) major forceps, 2) minor forceps, 3) genu of corpus callosum, 4) splenium of corpus callosum and GM, 5) head of caudate nucleus, and 6) thalamus.

The effects of Rayleigh noise were not taken into account, considering the high signal-to-noise ratio (SNR) present in all images used for T_2 estimation. More specifically, the minimum SNR in images from both sites ($SNR_{S1} \sim 15$: $SNR_{S2} \sim 19$) exceeds the threshold for approximate Gaussianity (SNR $>$ 3 [17] or SNR $>$ 8 [18]).

Quality Control

Data from both an American College of Radiology (ACR) (19) phantom and a human (a.k.a. living phantom) were collected periodically in order to assess the repeatability within and across sites. In accordance with the protocol of the overall study, the ACR phantom was nominally scanned with the full protocol at monthly intervals at both sites (total of 93 scans). The living phantom was a healthy adult male who was 53 years old at the beginning of the study and was scanned at approximately one-year intervals, also at both sites (total of 11 scans). This phantom enables a comparison of derived tissue characteristics (i.e., relaxation times, tissue volumes, etc.) that is not possible with the ACR phantom. Figures 1 and 2a illustrate the regions of interest (ROIs) where T_2 was measured in the phantoms and provide the expected T_2 relaxation time constants based on the literature and the known composition of the ACR phantom. In addition, for the ACR phantom, a 32-echo single-slice Carr-Purcell-Meiboom-Gill (CPMG) sequence (following the guidelines of Poon and Henkelman (15)) was used as a gold standard in assessing the accuracy of the estimates obtained with the relaxometry protocol used on the children.

Subject ROIs

Because the currently available stereotaxic brain models, such as the ICBM152 average (20), are based on adult brains, they are often not suitable as targets for registration of infant scans. The ability to create a standard model in which structures are distinctly and consistently defined for the entire infant population is hin-

dered by relative contrast differences due to a GM/WM contrast reversal around the age of 6 months. At this stage of maturation, there is poor GM/WM differentiation, adding further difficulty to reliable structural segmentation. Given these limitations, the relaxometry analysis in the subject cohort was restricted to manually selected ROIs with careful selection of areas free of partial volume effects. Since the aim is to include a single tissue type, the selection is carried out on the image that provides the highest contrast for a specific age. This often corresponds to the image acquired at TE = 112 msec and TE = 121 msec for the GE and Siemens sequences, respectively. The specified ROIs in Fig. 2b include four WM (minor forceps, major forceps, genu and splenium of corpus callosum) and two deep GM (head of caudate nucleus, thalamus) regions, each of which is relatively large and easily identifiable. Bilateral results were averaged.

Data Analysis

Based on previous work in modeling T_2 age dependence in young children (7,8), both mono- and biexponential fits were attempted. It is important to note that these models are applied to the T_2 change over time, which should not be confused with the monoexponential model used for T_2 estimation. The single exponential model is given by:

$$T_2 = T_{2(0)} + T_{2(1)}e^{-Ct}$$

$$where\ tT = Tage\ in\ months$$

$$T_{2(0)},\ T_{2(1)}e^{-Ct}\ are\ in\ seconds$$

$$C\ is\ in\ months^{-1}. \quad [2]$$

The biexponential model is similar, with two added parameters in the extra term:

$$T_2 = T_{2(0)} + T_{2(1)}e^{-Ct} + T_{2(1)}e^{-C_2t}$$

$$where\ t = age\ in\ months$$

$$T_{2(0)},\ T_{2(1)}, T_{2(2)}\ are\ in\ seconds$$

$$C_1\ and\ C_2\ are\ in\ months^{-1}. \quad [3]$$

The parameters were estimated using nonlinear Nelder-Mead minimization through the *fminsearch* function in MATLAB (The Mathworks, Inc., Natick, MA, USA). In addition, the adjusted coefficient of determination (R_a^2), which gives an indication of the reliability of the fit, was used to decide whether the extra exponential term was justified (7,8):

$$R_a^2 = 1 - \frac{\text{residual Mean Square}}{\text{total Mean Square}}$$

$$= 1 - \frac{\sum_1^n (Y_j - \hat{Y}_j)^2/n - m - 1}{\sum_1^n (Y_j - \bar{Y}_j)^2/n - 1} \quad [4]$$

where
$Y = Y_{observed}$ n = total number of data points
$\hat{Y} = Y_{predicted}$ m = number of independent variables in the regression model

Parameter standard deviations (SDs) were used to quantify the reliability of the estimated parameters, while the variance accounted for (VAF) was used to express the proportion of the variability in the observed data attributable to the dependence on the regression equation. The advantage of using the adjusted coefficient of determination (R_a^2) to determine whether added parameters are justified is that it takes into account the number of parameters and will only increase if these added parameters improve the fit. On the other hand, the VAF should be used in conjunction with an F-test as a measure of goodness of fit. An F-test was also performed to determine whether the four-echo and two-echo data could be combined. Directly computing the statistical difference between the two-point and four-point fits is difficult because not all age groups are well represented and only a limited number of scans were acquired at each site (S1: two echoes: 60 vs. four echoes: 31; S2: two echoes: 196 vs. four echoes: 57). Therefore, the analysis consisted of comparing the age regressions between the two-point fits for all data sets and including the four-point fits with the two-point fits. Because it is desirable to retain the higher-precision four-echo data, a weighted fit was also investigated. This weighting, based on the SD of estimated T_2 values in each ROI, was combined with a weighting based on subjects per age group. The difference in age distribution is especially apparent for S1 (Table 1).

RESULTS

Quality Control

The variability across time within each site is quite low (<5% and <8% for the ACR and living phantom, respectively), indicating good reproducibility. The estimates for the ACR phantom provided by the dual-echo TSE sequences are similar to but relatively higher than the gold-standard 32-echo CPMG sequence (ROI_1 $T_{2(TSE)}$ = 153.4 ± 5.3 msec, $T_{2(CPMG)}$ ~ 135 msec; ROI_2 $T_{2(TSE)}$ = 74.0 ± 2.7 msec, $T_{2(CPMG)}$ ~ 70 msec). This discrepancy can be attributed to the expected lower accuracy of the four-echo sequence as compared to the 32-echo gold standard. For the living phantom, the estimated values are relatively close to the expected range for healthy adults in both WM ($T_{2(S1)}$ = 78.9 ± 2.2 msec; $T_{2(S2)}$ = 91.1 ± 3.4 msec; $T_{2(adult)}$ ~ 87 msec [21]) and GM structures ($T_{2(S1)}$ = 87.6 ± 3.3 msec $T_{2(S2)}$ = 104.9 ± 7.6 msec; $T_{2(adult)}$ ~ 92 msec [21]). However, for both the ACR and living phantoms, the T_2 estimates from S1 are consistently lower than those of S2 ($P < 0.01$), probably due to systematic scanner differences.

Age Regression

The average T_2 relaxation constants at birth of the combined site data are significantly prolonged as compared to adult values in both WM (major and minor forceps: $T_{2(birth)}$ = 404.4 ± 8.1 msec, corpus callosum: $T_{2(birth)}$ = 228.6 ± 3.6 msec; $T_{2(adult)}$ ~ 80–90 msec) and GM

Table 2
Monoexponential Parameter Estimates for Separate and Combined Sites in Selected ROIs*

Parameter	Site	Major forceps	Minor forceps	Genu of corpus callosum	Splenium of corpus callosum	Caudate nucleus	Thalamus
$T_{2(0)}$ (msec)	S1	101 ± 1.0	100 ± 1.4	80.4 ± 0.85	85.1 ± 0.75	110 ± 0.67	104 ± 0.61
	S2	114 ± 0.88	112 ± 1.4	87.8 ± 0.76	93.9 ± 0.65	122 ± 0.50	117 ± 0.39
	C	111 ± 0.91	108 ± 1.2	86.5 ± 0.85	92.4 ± .73	119 ± 0.62	114 ± 0.55
$T_{2(1)}$ (msec)	S1	269 ± 12	227 ± 13	142 ± 4.3	128 ± 5.2	100 ± 5.5	92.7 ± 5.1
	S2	384 ± 6.1	376 ± 8.8	172 ± 2.3	149 ± 2.0	116 ± 2.0	116 ± 1.5
	C	301 ± 6.6	281 ± 7.4	147 ± 2.7	132 ± 2.9	103 ± 2.7	95.7 ± 2.6
C (1/month)	S1	0.30 ± 0.017	0.21 ± 0.016	0.16 ± 0.008	0.22 ± 0.014	0.35 ± 0.028	0.34 ± 0.026
	S2	0.32 ± 0.008	0.26 ± 0.009	0.17 ± 0.004	0.22 ± 0.007	0.34 ± 0.011	0.34 ± 0.010
	C	0.29 ± 0.010	0.22 ± 0.009	0.16 ± 0.010	0.22 ± 0.009	0.31 ± 0.016	0.33 ± 0.017
VAF (%)	S1	98.6	96.6	99.4	99.4	99.7	99.7
	S2	99.2	98.3	99.5	99.4	99.8	99.9
	C	98.3	97.1	98.9	98.9	99.5	99.6
R_a^2 (mono)	S1	0.93	0.80	0.94	0.94	0.93	0.93
	S2	0.95	0.91	0.95	0.93	0.94	0.95
	C	0.91	0.86	0.90	0.88	0.86	0.86
R_a^2 (bi)	S1	0.94	0.89	dnc	dnc	0.95	0.95
	S2	0.97	0.95	dnc	dnc	0.97	0.97
	C	0.92	0.87	dnc	dnc	0.86	dnc

*Fit parameter values are: parameter ± parameter SD.
S1 = site 1, S2 = site 2, C = both sites combined, VAF = variance accounted for, R_a^2 = adjusted coefficient of determination, mono = monoexponential model, bi = biexponential model, dnc = did not converge using *fminsearch* in MATLAB (The Mathworks, Inc., Natick, MA, USA).

($T_{2(birth)}$ = 215.9 ± 3.2 msec, $T_{2(adult)}$ ~ 90–100 msec). During the first few months a rapid decline in T_2 is observed, followed by a slower decrease. Because the progression with age is of particular interest in this study and a deviation between the intercepts of any regression curves does not correspond to an actual difference in the evolution of the T_2 parameter with age, the parameter C was used to compare the various regression lines. First, the combination of four- and two-echo data were investigated for each site. A two-tailed t-test revealed a significant difference for S1 in the thalamus ($t(87) = 2.1$, $P < 0.05$) and S2 in the caudate nucleus ($t(249) = 2.9$, $P < 0.01$), while the differences in all other ROIs were not significant (1: $t(87) < 1.9$, $P > 0.05$; 2: $t(249) < 1.6$, $P > 0.1$). The general lack of significance is to be expected, considering that only a limited number of subjects could withstand the acquisition of the second set of dual-echo images. In order to retain and give greater importance to the more reliable four-echo data, weighting based on the ROI SD was included. In addition, this helped to compensate for the reduced precision of the estimates of very high T_2 values, which were measured with relatively short TEs. A weighting based on age was also included so that each age group would be equally represented. This combined weighting was used for all further analysis.

In terms of results between the two sites, as in the case with the phantoms, the T_2 estimates from S1 were consistently lower compared to those from S2. Nonetheless, as mentioned above, the progression of T_2 with age is of greatest importance; therefore, parameter C was compared between the two sites. A two-tailed t-test revealed a significant difference in the minor forceps ($t(336) = 2.5$, $P < 0.02$) but failed to be significant in all other ROIs ($t(336) < 1.8$, $P > 0.10$). The discrepancy in the minor forceps is probably a result of the relatively low quality of fit for S1 ($R_a^2 = 0.80$). Nevertheless, because in general these results indicate a similar dependence on age for the two sites, the data sets were combined. The results from each of the sites and the parameter estimates of the combined data set, all weighted according to ROI variance and age group sizes, are given in Table 2 for all ROIs.

From these results, the quality of fit of the combined data to the monoexponential model is relatively high in all ROIs (R_a^2 = 86–91% [VAF = 97.1–98.9%] in WM; R_a^2 = 86% [VAF = 99.5%] in GM). Due to the variability between sites, the goodness of fit is in general slightly less for the combined data set than when a single site is considered ($R_a^2{}_{S1}$ = 80–94%; $R_a^2{}_{S2}$ = 91–95% in WM; $R_a^2{}_{S1}$ = 93%; $R_a^2{}_{S2}$ = 94–95% in GM). To determine whether additional parameters were justified, a biexponential model was tested. The combined data often failed to converge to the biexponential model and, as shown in Table 2, the coefficient of determination did not increase substantially (maximum increase in R_a^2 of 1%). Thus a monoexponential is sufficient and best suited to the data. An F-test revealed no significant difference in the regression parameters with gender ($P < 0.01$). The resulting plots are shown in Fig. 3 for each anatomical ROI. The crossover in T_2 values between cerebral WM and deep GM occurs at approximately 15 months of age. In terms of the significance of the estimated parameters, $T_{2(0)}$ corresponds to the relaxation time at ~4.5 years, at which point relaxation parameters are thought to be approaching their adult value. This is reflected in the results (WM: $T_{2(0)}$ = 86.5–111 msec, $T_{2(adult)}$ ~ 87 msec [21]; GM: $T_{2(0)}$ = 114–119 msec, $T_{2(adult)}$ ~ 92 msec [21]). The estimated values are a little higher than expected, which may be partly due to the sequence-specified *effective* TEs and because at 4.5

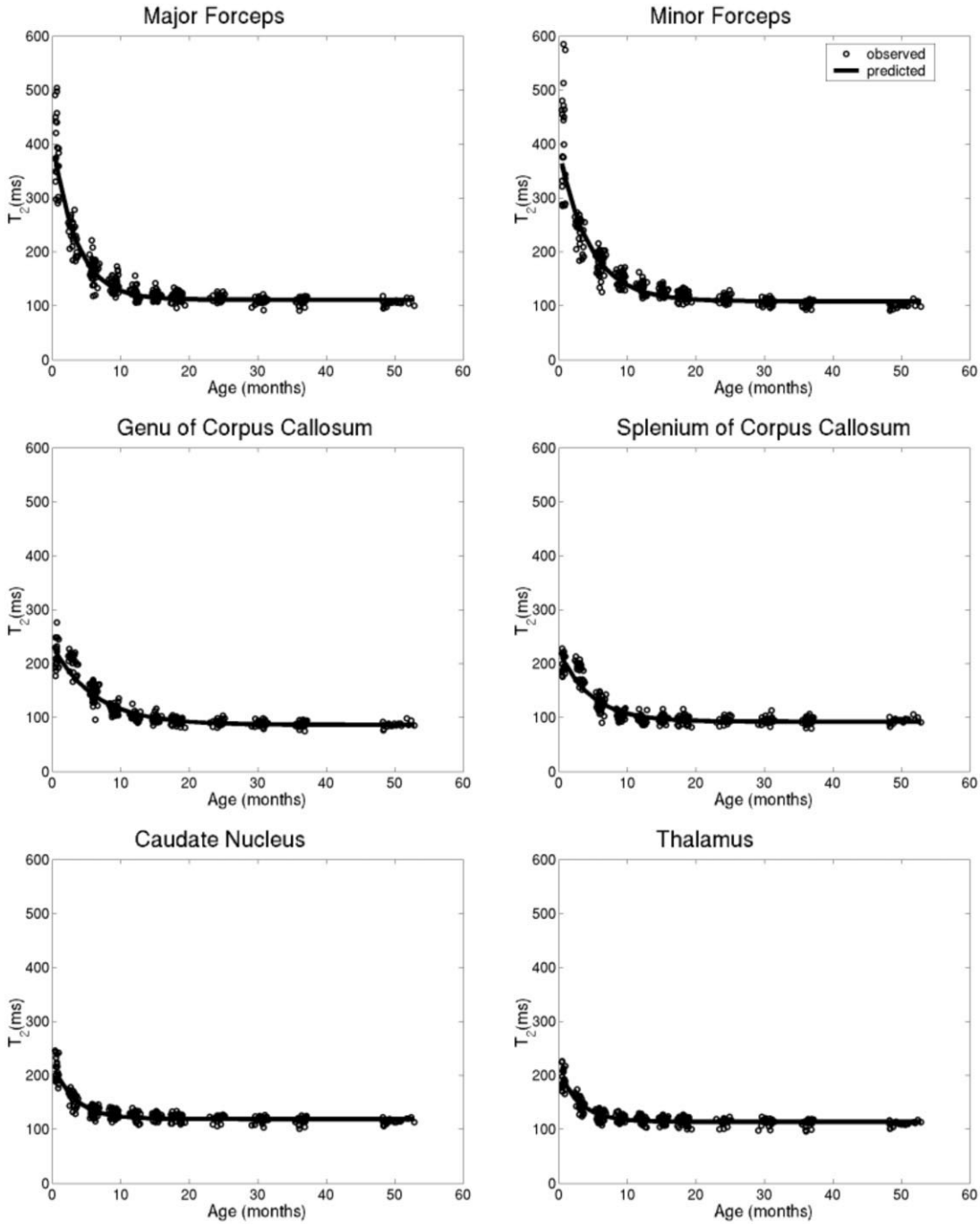

Figure 3. Monoexponential regression of T_2 with age in selected ROIs.

years, full maturation may not yet be reached. A faster progression in T_2 values is observed in the major compared to the minor forceps ($C_{MF} \sim 0.29$ months^{-1}, $C_{mf} \sim 0.22$ months^{-1}), and faster in the splenium compared to the genu of the corpus callosum ($C_{CCs} \sim 0.22$ months^{-1}, $C_{CCg} \sim 0.16$ months^{-1}). For deep GM, the rates of change are $C_{cn} \sim 0.31$ months^{-1} and $C_{thal} \sim 0.33$ months^{-1} for the caudate nucleus and the thalamus respectively.

DISCUSSION

Based on the results for both the ACR and living phantom, the relaxation parameter estimates show good reproducibility over time (SD < 8%) and are within 12% (ROI_1) and 5% (ROI_2) of the values obtained by gold-standard methods (applied on the ACR phantom). The fact that the estimates for the shorter T_2 (74 ± 2.7 msec) in ROI_2 are in better agreement with the gold-standard data (~70 msec) is probably due to the choice of TEs in the protocol. In addition to the expected loss in estimate accuracy from a four-echo vs. a 32-echo sequence, the shorter maximum TE of the TSE sequence ($TE_{max(TSE)}$ = 165 msec vs. $TE_{max(CPMG)}$ = 259 msec) may account for the increased discrepancy in estimating the longer T_2 values in ROI_1 ($T_{2(TSE)}$ = 153.4 ± 5.3 msec, $T_{2(CPMG)} \sim$ 135 msec). There is also a consistent T_2 estimate bias

between the two sites, by which values from S2 are higher than those from S1. This is probably a result of systematic differences between the GE and Siemens scanners. More specifically, the multiple slice-selective refocusing pulses, which are characteristic of 2D-FT, multislice imaging techniques, have transition zones in which the flip angles vary from nominally 180° to 0°. With these nonideal pulses, resulting from either B_1-field nonuniformity or slice-profile imperfections, stimulated echoes with T_1 rather than T_2 decay constants will contribute to the measured signal intensities at the different TEs in a manner that depends on the precise slice profiles. These effects will undoubtedly vary from manufacturer to manufacturer. Nonetheless, the expected range of relaxation time constants during infancy far exceeds the variability in the phantom studies over time, so that the overall observations should be quite robust. In addition, despite the difference in T_2 estimates, the progression with age is in general consistent in all ROIs and it is thus reasonable to combine the data from the two sites for this particular analysis. Although this provides support for system independence, it does not guarantee it, and careful consideration is required when combining multisite data.

There is inevitably a trade-off between accuracy and speed in terms of relaxometry acquisition sequences. For example, to achieve a similar resolution, a single-slice 32-echo acquisition would require close to six minutes of scan time, whereas a full-brain four-echo acquisition requires at most 10 minutes. In the context of this study, precision and brain coverage were deemed more important than accuracy, such that results should be reproducible and robustly capture changes with time but need not necessarily capture the exact time constant value. Moreover, scanning a population of unsedated children in the birth to less than 5-year age range necessitates very short scan times. The time limitations also preclude the use of multicomponent T_2 analysis, which would require at least 32 TEs and sufficient SNR to reliably differentiate relaxation components.

The average T_2 relaxation parameters at birth in the current study for the minor (S1: $T_{2(mf)} = 372 \pm 66$ msec; S2: $T_{2(mf)} = 476 \pm 64$ msec) and major (S1: $T_{2(MF)} = 352 \pm 44$ msec; S2: $T_{2(MF)} = 464 \pm 33$ msec) forceps are comparable with the values obtained by Ding et al (8) at 1.5T in WM (~400 msec). Similarly for GM, the current results in the caudate nucleus (S1: $T_{2(cn)} = 197 \pm 9.5$ msec; S2: $T_{2(cn)} = 233 \pm 10$ msec) and the thalamus (S1: $T_{2(thal)} = 183 \pm 9.0$ msec; S2: $T_{2(thal)} = 214 \pm 8.5$ msec) are consistent with those reported by Ding et al (8) (~200 msec). Because an unexpected decrease in the T_2 relaxation parameter has been observed with increasing field strength (22,23), our results are also qualitatively comparable to those obtained at a higher field strength. For example, T_2 values obtained by Ferrie et al (6) at 2.35T in healthy preterm newborns are shorter but in the same relative order as those for the current study ($T_{2(mf)} = 266 \pm 35$ msec; $T_{2(MF)} = 213 \pm 28$ msec; $T_{2(cn)} = 172 \pm 10$ msec; $T_{2(thal)} = 120 \pm 6$ msec). The relatively lower SDs reported (6) can be explained by the very restricted cohort investigated (seven subjects at a postconceptional age of 37 weeks). In the present study, the gestational age was not provided and thus a greater variability between subjects is expected. A similar argument applies to the results shown by Thornton et al (10) at 2.4T ($T_{2(mf)} = 228 \pm 32$ msec; $T_{2(occipital\ WM)} = 217 \pm 33$ msec; $T_{2(thal)} = 136 \pm 13$ msec), where the subject cohort was limited to an age range of 37–42 weeks postconception. A consistent result in these studies and the present study is that the T_2 value of WM at birth significantly exceeds that of GM. While earlier relaxometry studies failed to detect this difference (5,9,24), it was argued by Ding et al (8) that the results were affected by relatively short TRs on the order of 2000–2500 msec, as opposed to the 3000–4500 msec TRs used in later studies. This refers to the potential leftover T_1 signal component, which is relatively long-lived in neonates ($T_{1(max)} \sim 2.5$ s). However, we expect the effect of this residual magnetization to be minimal in our study. A more likely explanation is that the short TEs in earlier reports ($TE_{max} = 56$ msec [5]; 80 msec [9]; 90 msec [24]), used to measure the relatively long T_2s expected for this age range, may be inadequate. Using longer TEs (two-echo: $TE_{max} = 121$ msec; four-echo: $TE_{max} = 165$ msec for the present protocol) effectively allows sufficient magnetization decay and thus more accurately captures infant T_2 relaxation times, which are on the order of 400 msec.

For the age range of the present study, a significant decrease in the T_2 relaxation parameter is characterized by a steep decline within the first year, followed by a less pronounced decline thereafter. Thus, in accordance with a previous study (7), monoexponential regressions with age were applied, providing high-quality fits. In general, the monoexponential fit was well suited to T_2 (mean $R_a^2 \sim 88\%$) and fits were slightly better in WM ($R_a^2 = 86$–91%) than in GM ($R_a^2 = 86\%$). A biexponential model, as proposed by Ding et al (8), was also tested but failed to be justified for our data set, which had a more restricted age range (<5 years) than the previous study (<40 years) (8). Thus, insufficient data from older subjects may impede the detection of a second exponential term, which is thought to reflect the subtle changes extending into adult age (25,26).

The expected result was obtained for relaxation parameters for subjects approaching 4 years 5 months (the upper age limit in the cohort) in that they begin to approach the adult range and the T_2 value of GM exceeds that of WM (as expressed through the $T_{2(0)}$ parameter). The relaxation parameters are shown to exhibit a rapid decline until approximately 1 year of age, at which point the values reach the range expected for adults. This result is qualitatively comparable to the 10-month rapid decrease reported by Ding et al (8), but shorter than the 2- to 3-year period observed by Ono et al (24) (both studies were carried out at 1.5T). The discrepancy with the latter results is probably due to the relatively short TEs (TE = 40, 80 msec) used by Ono et al (24) and the difference in the definition of the point at which values "approach" the adult range. Other reports have shown that the significant lengthening in relaxation times as compared to adults extends to 3–4 years at 0.15T (9) and 0.35T (5). The difference in sequence, field strength, and TEs could be the source of the discrepancies.

Our data also show a first crossover between relaxation parameters of WM and GM (splenium of corpus callosum and caudate nucleus) at approximately 6 months, followed by one at approximately 13 months (between the major forceps and the caudate nucleus). These results approach the crossover at ~7 months found by Ding et al (8) between similar structures (frontal lobe WM and caudate nucleus). The difference could be due to the fact that these estimates were derived from a monoexponential model in our case and a biexponential model in the case of Ding et al (8). Also, as is the case for all the comparisons made thus far, the choice of the ROIs is an additional source of discrepancies among studies. Since there is no available standard model for pediatric brains, regions are selected manually and therefore are subject to interrater variability and partial volume effects.

Throughout the literature, the generalized rapid decrease in relaxation parameters for WM and GM is thought to be primarily indicative of water content and distribution changes. Several studies have confirmed that the steep decline in water content during early childhood is paralleled by pronounced decreases in T_2 values within the first year postnatal, with more subtle but continual decreases extending into adulthood (5,27,28). Concurrent with water content decline, WM myelination occurring during early development affects the relaxation parameters through alterations of brain water distribution. The increase in concentration of myelin precursors, such as myelin basic proteins, cholesterol, and glycolipids (29), as well as the proliferation and differentiation of glial cells and the development of axons and dendrites (24,30), increase the binding potential for protons of free water molecules to the surrounding macromolecules and effectively reduce the observed relaxation times (31,32). From postmortem studies, and paralleled by qualitative and quantitative MRI studies, it has been shown that myelination progresses most rapidly until 2 years of age, followed by a slower and less dramatic change extending well into the second decade of life (28,33). This temporal progression is reflected in the results of this study, where T_2 relaxation times exhibit a rapid decline until about 1 year of age in all ROIs, at which point the values are within approximately 10% of the estimate at the age of 4 years 5 months. The average decay rate in each type of tissue as a whole is 0.19 ± 0.01 month^{-1} in the corpus callosum, 0.26 ± 0.01 months^{-1} in WM, and 0.32 ± 0.02 months^{-1} in GM. In terms of the general spatial progression, the rate of decline for T_2 values with age is faster in the major forceps compared to the minor forceps ($C_{MF} = 0.29 \pm 0.010$ months^{-1} > $C_{mf} = 0.22 \pm 0.009$ months^{-1}) and similarly more rapid in the splenium than in the genu of the corpus callosum ($C_{CCs} = 0.22 \pm 0.009$ months^{-1} > $C_{CCg} = 0.16 \pm 0.010$ months^{-1}).

These relative rates are consistent with the results of Ding et al (8) and with the expected posterior–anterior pattern of myelination. This is evidenced through perinatal histochemical studies (33) and paralleled through qualitative analysis (2–4), measures of quantitative relaxometry (7,8), magnetization transfer experiments (34), and estimates of full brain cholesterol (28). In fact, during early brain development, myelination is initiated caudally, in the spinal cord, and spreads rostrally through the brain. Another interesting observation is the apparent slower rate of decline in the corpus callosum as compared to more peripheral WM structures ($C_{CC} \sim 0.19$ months^{-1} < $C_{peripheralWM} \sim 0.26$ months^{-1}). This may reflect a more advanced degree of myelination in the deeper WM structures (35), such as a relatively high concentration of early myelinating fibers. Thus, at birth the process is already nearing maturation and exhibits a slower evolution with time (34).

The average rate of decline in deep GM is considerably faster than that in peripheral and deep WM structures ($C_{cn} \sim 0.31$ months^{-1}, $C_{thal} \sim 0.33$ months^{-1} vs. $C_{pWM} \sim 0.26$ months^{-1} and $C_{CC} \sim 0.19$ months^{-1}). This contradicts the rate constants of the first exponential term in the model proposed by Ding et al (8) for the same structures ($C1_{cn} \sim 0.40$ months^{-1}, $C1_{thal} \sim 0.31$ months^{-1} vs. $C_{pWM} \sim 0.48$ months^{-1}). It appears that this difference is related to the choice of model and weighting. For example, for the unweighted data that did converge to the biexponential model (major/minor forceps and caudate nucleus), the decay constant from the first exponential term for WM ($C_{pWM} \sim 0.53$ months^{-1}) is greater than that for GM ($C_{cn} \sim 0.45$ months^{-1}). However, the data in general did not converge to the biexponential model and no significant increase in the adjusted coefficient of determination was observed.

The main cause of the decay in GM is attributed to decreases in water content, concurrent with the rapid proliferation and formation of oligodendroglial cells, synapses, and dendrites, which further reduces the free water in GM (36,37). It has been suggested that another possible factor contributing to T_2 reductions in deep GM structures is the accumulation of paramagnetic metals, such as iron (38,39), as well as the presence of myelinated WM projections in regions such as the thalamus.

In conclusion, in accordance with the objective of the NIH MRI Study of Normal Brain Development, normal age-related changes in T_2 relaxometry were investigated and shown to provide a sensitive index for the assessment of normal brain maturation through relaxation time constants that reflect the alterations in water content and distribution. Of special interest is the progression of myelination in WM, which is the dominant developmental process that occurs in synchrony with the observed relaxation parameter decline. During the neonatal period, the changes are especially dramatic, as demonstrated by the rapid shortening of this parameter and modeled by a rapid monoexponential decay with age. The culmination of the results to date represents a subset of a normative database, a portion of which is currently available online (http://www.NIH-PediatricMRI.org), and the remainder of which will become publicly available in the future. This will provide a comparison standard for other studies investigating normal brain development, as well as studies of relaxation parameter deviations associated with disease. Neural-behavioral data, collected concurrently with the MR data, will also allow for the investigation of a potential relationship between brain T_2 and behavioral functions.

ACKNOWLEDGMENTS

We thank the NIH contracting officers for their support. We also acknowledge the important contribution and remarkable spirit of John Haselgrove, PhD (deceased). The views expressed in this article do not necessarily represent the official views of the National Institute of Mental Health, the National Institute of Child Health and Human Development, the National Institute on Drug Abuse, the National Institute of Neurological Disorders and Stroke, the National Institutes of Health, the U.S. Department of Health and Human Services, or the United States government.

The Brain Development Cooperative Group is composed of the following investigators from the pediatric study centers. *Children's Hospital, Boston, MA, USA:* Principal Investigator, Michael J. Rivkin, MD; Investigators, Deborah Waber, PhD; Robert Mulkern, PhD; Sridhar Vajapeyam, PhD; Peter Davis, BS; Julie Koo, BS; Sandra Kosta, BA; Jacki Marmor, MA; Richard Robertson, MD; Heidelise Als, PhD; and Gloria McAnulty, PhD. *Washington University, St. Louis, MO, USA*: Principal Investigator, Robert C. McKinstry, MD, PhD; Co-Principal Investigator, C. Robert Almli, PhD; Investigators, Aaron A. Wilber, MS; Asif Moinuddin, MD; Tina M. Day, BA; Jennifer L. Edwards, MSW; Suzin J. Blankenship, BA; Clinical Coordinating Center at Washington University, Principal Investigator: Kelly Botteron, MD; Investigators, C. Robert Almli, PhD; Cheryl Rainey, BS; Stan Henderson, MS; Tomoyuki Nishino, MS; William Warren; Jennifer L. Edwards, MSW; Diane Dubois, RN; Karla Smith; and Tish Singer. *Data Coordinating Center, McGill University, Montreal, Quebec, Canada*: Principal Investigator, Alan C. Evans, PhD; Investigators, Rozalia Arnaoutelis, BS; G. Bruce Pike, PhD; D. Louis Collins, PhD; Gabriel Leonard, PhD; Tomas Paus, MD; Alex Zijdenbos, PhD; and Research Staff, Samir Das, BS; Vladimir Fonov, PhD; Luke Fu, BS; Jonathan Harlap; Ilana Leppert, MEng; Denise Milovan, MA; Dario Vins, BC. *Georgetown University, Washington, DC, USA:* Thomas Zeffiro, MD, Ph.D; and John Van Meter, PhD. *Harvard University/McLean Hospital, Boston, MA, USA*: Nicholas Lange, ScD, is a biostatistical study design and data analysis investigator at the Data Coordinating Center. *Diffusion Tensor Processing Center, National Institutes of Health, Bethesda, MD, USA:* Principal Investigator, Carlo Pierpaoli, MD, PhD; Investigators, Peter J. Basser, PhD; Lin-Ching Chang, ScD; and Chen Guan Koay, PhD; and Lindsay Walker, MS; Principal NIH Collaborators: Lisa Freund, PhD (NICHD); Judith Rumsey, PhD (NIMH); Lauren Baskir, PhD (NIMH); Laurence Stanford, PhD (NIDA); Karen Sirocco, PhD (NIDA); Katrina Gwinn-Hardy, MD (NINDS); and Giovanna Spinella, MD (NINDS). *Spectroscopy Processing Center, University of California, Los Angeles, Los Angeles, CA, USA:* Principal Investigator, James T. McCracken, MD; Investigators, Jeffry R. Alger, PhD; Jennifer Levitt, MD; and Joseph O'Neill, PhD.

REFERENCES

1. Paus T, Collins DL, Evans AC, Leonard G, Pike B, Zijdenbos A. Maturation of white matter in the human birth: a review of magnetic resonance studies. Brain Res Bull 2001;54:255–266.
2. Takeda K, Nomura Y, Sakuma H, Tagami T, Okuda Y, Nakagawa T. MR assessment of normal brain development in neonates and infants: comparative study of T1- and diffusion-weighted images. J Comput Assist Tomogr 1997;21:1–7.
3. Van der Knaap MS, Valk J. MR imaging of the various stages of normal myelination during the first year of life. Neuroradiology 1990;31:459–470.
4. Ashikaga R, Araki Y, Ono Y, Nishimura Y, Ishida O. Appearance of normal brain maturation on fluid-attenuated inversion-recovery (FLAIR) MR images. AJNR Am J Neuroradiol 1999;20:427–431.
5. Holland B, Haas D, Norman D, Brant-Zawadski M, Newton TH. MRI of normal brain maturation. AJNR Am J Neuroradiol 1986;7:201–208.
6. Ferrie J, Baratin L, Saliba E, et al. MR assessment of the brain maturation during the perinatal period: quantitative T2 MR study in premature newborns. Magn Reson Imaging 1999;17:1275–1288.
7. Engelbrecht V, Rassek M, Preiss S, Wald C, Mödder U. Age-dependent changes in magnetization transfer contrast of white matter in the pediatric brain. AJNR Am J Neuroradiol 1998;19:1923–1929.
8. Ding X, Kucinski T, Wittkugel O, et al. Normal brain maturation characterized with age-related T2 relaxation times: an attempt to develop a quantitative imaging measure for clinical use. Invest Radiol 2004;39:740–746.
9. Masumura M. Proton relaxation time of immature brain: II. In vivo measurement of proton relaxation time (T1 and T2) in pediatric brain by MRI. Child Nerv Syst 1987;3:6–11.
10. Thornton JS, Amess PN, Penrice J, Chong WK, Wyatt JS. Cerebral tissue water spin-spin relaxation times in human neonates at 2.4 Tesla: methodology and the effects of maturation. Magn Reson Imaging 1999;17:1289–1295.
11. National Institutes of Health. The MRI Study of Normal Brain Development. Protocol: October 2004. Available at: http://www.bic-.mni.mcgill.ca/nihpd/info. Last accessed: October 28, 2008.
12. Almli CR, Rivkin MJ, McKinstry RC. Brain Development Cooperative Group. The NIH MRI study of normal brain development (Objective-2): newborns, infants, toddlers, and preschoolers. Neuroimage 2007;35:308–325.
13. United States Census Bureau. Basic counts: population. Available at: http://factfinder.census.gov/servlet/SAFFPeople?_sse=on. Last accessed: October 28, 2008.
14. Evans AC; Brain Development Cooperative Group. The NIH MRI Study of Normal Brain Development. Neuroimage 2006;30:184.
15. Poon C, Henkelman RM. T2 quantification for clinical applications. J Magn Reson Imaging 1992;2:541–553.
16. Mackay A, Whittall K, Adler J, Li D, Paty D, Graeb D. In vivo visualization of myelin water in brain by magnetic resonance imaging. Magn Reson Med 1994;31:673–677.
17. Nowak RD. Wavelet-based Rician noise removal for magnetic resonance imaging. IEEE Trans Image Process 1999;8:1408–1419.
18. Henkelman R. Measurement of signal intensities in the presence of noise in MR images. Med Phys 1985;12:232–233.
19. Clarke GD. Phantom test guidance for the ACR MRI accreditation program and phantom site scanning instruction guide. Reston, VA: American College of Radiology; 2000. 22 p.
20. Mazziotta JC TA, Evans A, Fox P, Lancaster J. A probabilistic atlas of the human brain: theory and rationale for its development. The International Consortium for Brain Mapping (ICBM). Neuroimage 1995;2:89–101.
21. Zhou J GX, van Zijl PC, Silvennoinen MJ, Kauppinen R, Pekar J, Kraut M. Inverse T(2) contrast at 1.5 Tesla between gray matter and white matter in the occipital lobe of normal adult human brain. Magn Reson Med 2001;46:401–406.
22. Cremillieux Y, Ding S, Dunn JF. High-resolution in vivo measurements of transverse relaxation times in rats at 7 Tesla. Magn Reson Med 1988;39:285–290.
23. Brooks DJ, Luthert P, Gadian D, Marsden CD. Does signal-attenuation on high-field T2-weighted MRI of the brain reflect regional cerebral iron deposition? Observations on the relationship between regional cerebral water proton T2 values and iron levels. J Neurol Neurosurg Psychiatry 1989;52:108–111.
24. Ono J, Kodaka R, Imai K, et al. Evaluation of myelination by means of the T2 value on magnetic resonance imaging. Brain Dev 1993; 15:433–438.

25. Pfefferbaum A, Mathalon DH, Sullivan EV, Rawles JM, Zipursky RB, Lim KO. A quantitative magnetic resonance imaging study of changes in brain morphology from infancy to late adulthood. Arch Neurol 1994;51:874–887.
26. Hayakawa K, Konishi Y, Kuriyama M, Konishi K, Matsuda T. Normal brain maturation in MRI. Eur J Radiol 1991;12:208–215.
27. Miot-Noirault E, Barantin L, Akoka S, Le Pape A. T2 relaxation time as a marker of brain myelination: experimental MR study in two neonatal animal models. J Neurosci Methods 1997;72:5–14.
28. Dobbing J, Sands J. Quantitative growth and development of human brain. Arch Dis Child 1973;48:757–767.
29. Tower DB, Bourke RS. Fluid compartmentation and electrolytes of cat cerebral cortex in vitro. 3. Ontogenetic and comparative aspects. J Neurochem 1966;13:1119–1137.
30. Marthur-de Vré R. Biomedical implications of the relaxation behavior of water related to NMR imaging. Br J Radiol 1984;57:955–976.
31. Barkovich AJ, Kjos BO, Jackson DE, Norman D. Normal maturation of the neonatal infant brain: MR imaging at 1.5T. Radiology 1988;166:173–180.
32. Dietrich RB, Bradley WG, Zagaroza EJ, et al. MR evaluation of early myelination patterns in normal and developmentally delayed infants. AJR Am J Roentgenol 1988;150:889–896.
33. Yakolev PI, Lecours AR. The myelogenic cycles of regional maturation of the brain. In: Minkowski A, editor. Regional development of the brain in early life. Oxford: Blackwell; 1967. p 3–69.
34. Rademacher J, Engelbrecht V, Bürgel U, Freund HJ, Zilles K. Measuring in vivo myelination of human white matter fiber tracts with magnetization transfer MR. Neuroimage 1999;9:393–406.
35. Van der Knaap MS, Valk J. Myelin and white matter. In: Van der Knaap MS, Valk J, editors. Magnetic resonance of myelin, myelination and myelin disorders, 2nd ed. Berlin: Springer-Verlag; 1995. p 1–17.
36. Korogi Y, Takahashi M, Sumi M, et al. MR signal intensity of the perirolandic cortex in the neonate and infant. Neuroradiology 1996;38:578–584.
37. Pouwels PJ, Brockmann K, Kruse B, et al. Regional age dependence of human brain metabolites from infancy to adulthood as detected by quantitative localized proton MRS. Pediatr Res 1999;46:474–485.
38. Hallgren B, Sourander P. The effect of age on the non-haemin iron in the human brain. J Neurochem 1958;3:41–51.
39. Aoki S, Okada Y, Nishimura K, et al. Normal deposition of brain iron in childhood and adolescence: MR imaging at 1.5 T. Radiology 1989;172:381–385.